JACS
JOURNAL OF THE AMERICAN CHEMICAL SOCIETY
pubs.acs.org/JACS
Article

Platform for High-Spin Molecules: A Verdazyl-Nitronyl Nitroxide Triradical with Quartet Ground State

Evgeny V. Tretyakov,* Pavel V. Petunin,* Svetlana I. Zhivetyeva, Dmitry E. Gorbunov, Nina P. Gritsan,* Matvey V. Fedin, Dmitri V. Stass, Rimma I. Samoilova, Irina Yu. Bagryanskaya, Inna K. Shundrina, Artem S. Bogomyakov, Maxim S. Kazantsev, Pavel S. Postnikov, Marina E. Trusova, and Victor I. Ovcharenko*

Cite This: J. Am. Chem. Soc. 2021, 143, 8164–8176

ABSTRACT: Thermally resistant air-stable organic triradicals with a quartet ground state and a large energy gap between spin states are still unique compounds. In this work, we succeeded to design and prepare the first highly stable triradical, consisting of oxoverdazyl and nitronyl nitroxide radical fragments, with a quartet ground state. The triradical and its diradical precursor were synthesized via a palladium-catalyzed cross-coupling reaction of diiodoverdazyl with nitronyl nitroxide-2-ide gold(I) complex. Both paramagnetic compounds were fully characterized by single-crystal X-ray diffraction analysis, superconducting quantum interference device magnetometry, EPR spectroscopy in various matrices, and cyclic voltammetry. In the diradical, the verdazyl and nitronyl nitroxide centers demonstrated full reversibility of redox process, while for the triradical, the electrochemical reduction and oxidation proceed at practically the same redox potentials, but become quasi-reversible. A series of high-level CASSCF/NEVPT2 calculations was performed to predict inter- and intramolecular exchange interactions in crystals of di- and triradicals and to establish their magnetic motifs. Based on the predicted magnetic motifs, the temperature dependences of the magnetic susceptibility were analyzed, and the singlet−triplet (135 ± 10 cm^{-1}) and doublet-quartet (17 ± 2 and 152 ± 19 cm^{-1}) splitting was found to be moderate. Unique high stability of synthesized verdazyl-nitronylnitroxide triradical opens new perspectives for further functionalization and design of high-spin systems with four or more spins.

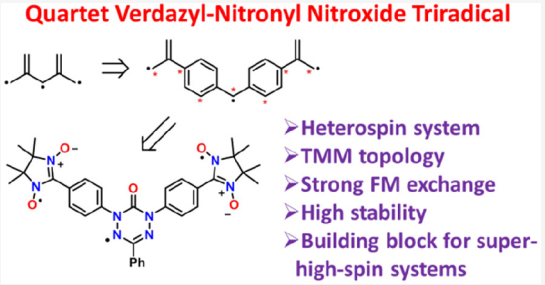

INTRODUCTION

π-Conjugated purely organic high-spin molecules (di- and polyradicals) with substantial intramolecular exchange interactions and intriguing magnetic properties have a significant potential for advanced technological applications and fundamental science.[1−5] The stable di- and polyradicals are considered as working elements of spintronic devices,[6−8] multifunctional molecule-based magnetic materials, and quantum machines.[9,10] Guidelines for the design of such high-spin molecules with exchange-coupled stable radical moieties have been developed using molecular orbital[11−15] and valence bond[16,17] theories. Based on these recommendations, a number of diradicals with *m*-phenylene or alkylidene bridging units with strong ferromagnetic interaction between radical parts and stability at room temperature have been designed.[18−26] Despite the obvious breakthrough in the chemistry of diradicals with a large energy gap between the high-spin ground state and low-spin excited state, air-stable tri- and polyradicals are still exotic compounds.

Previously reported examples of thoroughly characterized organic triradicals with a quartet ground state are shown in Figure 1. Polychlorinated triradical **1** is the only one representative of carbon-based triradical, where chlorine atoms prevent dimerization and restrict rotation of aryl groups owing to steric hindrance.[27] Triradical **1** is stable in air up to 250 °C; it was isolated as two stereoisomers with C_2 and D_3 symmetries. Magnetic measurements have revealed that the energy gap between the quartet ground state and the lowest energy doublet state ($\Delta E_{DQ}/k$) exceeds 290 K for both forms. Among annulated hydrazyls, 1,3,5-trisverdazyl-benzene (**2**) has been prepared as black prisms decomposing at 242−243 °C.[28] It has been shown that the quartet and doublet states of triradical **2** are equally populated in the temperature range from 230 to 340 K.

The greatest success in the synthesis of triradicals with a quartet ground state has been achieved for nitroxides, which

Received: March 18, 2021
Published: May 21, 2021

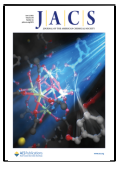

https://doi.org/10.1021/jacs.1c02938
J. Am. Chem. Soc. 2021, 143, 8164−8176

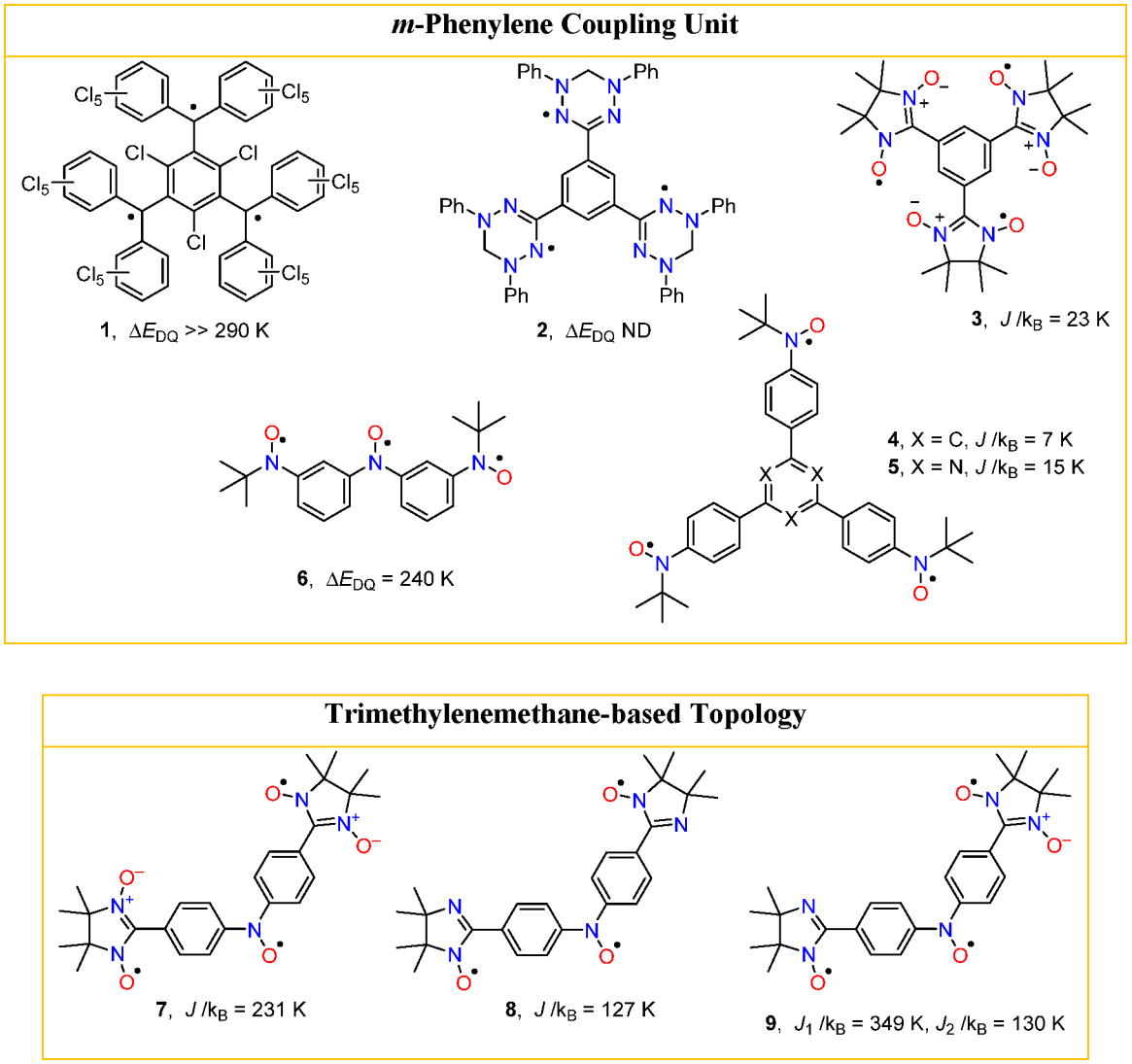

Figure 1. Previously reported air-stable organic triradicals with a quartet ground state.

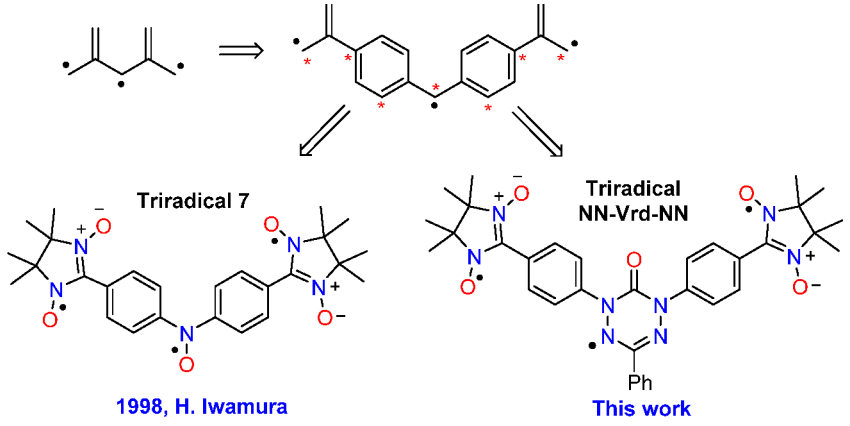

Figure 2. Step-by-step design of triradicals **7** and **NN-Vrd-NN** using ethylene-1,1-diyls as coupling units.

can be purified by column chromatography and applied as well-defined high-spin units for metal complexation.[29,30] In crystals of the first nitronyl nitroxide (NN) triradical **3** (ref 31; Figure 1), intramolecular exchange interactions have been overlapped with intermolecular antiferromagnetic interactions. To estimate the intramolecular magnetic coupling, a mixed crystal of **3** with 1,3,5-trinitrobenzene (**3**·TNB, 1:1) was prepared. Superconducting quantum interference device (SQUID) magnetometry of **3**·TNB has proved the intramolecular ferromagnetic interactions with J/k_B = 23 K.[32−34] The intramolecular ferromagnetic coupling is quite weak due to the small spin population of the C(2) atom in the NN part.

https://doi.org/10.1021/jacs.1c02938
J. Am. Chem. Soc. 2021, 143, 8164−8176

Scheme 1. Synthesis of Diradical I-Vrd-NN and Triradical NN-Vrd-NN

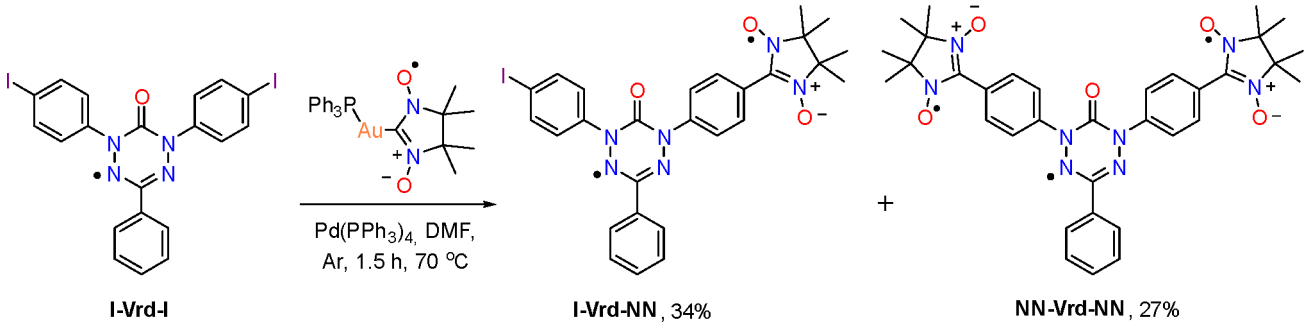

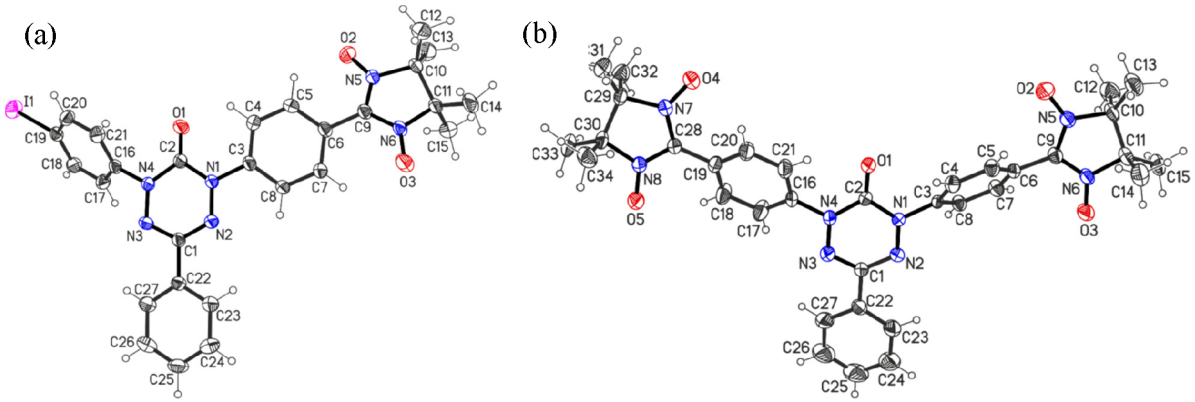

Figure 3. ORTEP views of diradical **I-Vrd-NN** (a) and triradical **NN-Vrd-NN** (b). Thermal ellipsoids are drawn at the 50% probability level.

Similar weak intramolecular exchange interactions with J/k_B = 6.8−15.3 K have been observed in *tert*-butyl nitroxide triradicals **4** and **5**.[35−37] The shortening of linkers between the paramagnetic centers has led to a significant increase in the exchange interaction parameters. Thus, in triradical **6**, the energy gap between the quartet ground and the lowest excited doublet states is reported to be 240 K.[38] Finally, the magnetic measurements of mixed triradicals **7** and **8** have clearly proved quartet ground states with J/k_B = 231 and 127 K, respectively.[19]

In the current work, we present a new type of triradical (**NN-Vrd-NN**, Figure 2) as a verdazyl (Vrd)-containing analog of compound **7** (Figure 1). Replacing the nitroxide moiety with Vrd is justified due to higher stability and a great potential for structure modification. In addition to the obvious possibility of conversion of the NN group into an iminonitroxide one, the **NN-Vrd-NN** triradical contains one more phenyl substituent suitable for addition of functional groups including paramagnetic centers. This property allows us to regard the **NN-Vrd-NN** triradical as a platform for the design of high-spin polyradicals. To create such molecules, it is important for future research to investigate intramolecular exchange interactions in **NN-Vrd-NN**.

Here, we report the synthesis, molecular and crystal structure, and magnetic properties of air-stable triradical **NN-Vrd-NN** and its diradical precursor **I-Vrd-NN**. Analysis of temperature dependence of magnetic susceptibility and pulse EPR-detected transient nutations confirmed the triplet and quartet ground states of the diradical and triradical, respectively.

RESULTS AND DISCUSSION

Our approach to the synthesis of triradical **NN-Vrd-NN** is related to the previously reported pathway for the **Vrd-NN** diradicals with a triplet ground state, proving the high stability of 6-oxoverdazyls in reaction conditions.[26] It was demonstrated[26] using spin alternation rule,[39,40] quantum chemical calculations and SQUID magnetometry that both the *para*-phenylene bridging by N1 or N5 nitrogen atoms of Vrd and *meta*-phenylene bridging by C3 carbon atom of Vrd lead to the triplet ground state of the **Vrd-NN** diradicals. To get the high-spin ground state, diradical **I-Vrd-NN** and triradical **NN-Vrd-NN** were also designed using *para*-phenylene bridging connected to nitrogen atoms. The synthesis of di- and triradical were performed via a palladium-catalyzed cross-coupling reaction of novel diiodoverdazyl **I-Vrd-I** with a gold(I) nitronyl nitroxide-2-ide complex Ph_3P-Au-NN[41,42] (Scheme 1, Experimental Section, and Supporting Information Section S1).

Mixtures of **I-Vrd-NN** and **NN-Vrd-NN** were formed in all experiments, and the best result was achieved under the heating of diiodoverdazyl **I-Vrd-I** (1 equiv) and Ph_3P-Au-NN (1.5 equiv) with 10 mol % of $Pd(PPh_3)_4$ in dimethylformamide (DMF) in an inert atmosphere. Analytically pure samples of the di- and triradical were isolated by column chromatography on silica followed by recrystallization from an *n*-heptane-acetone mixture. This system was also applied for crystal growth.

Crystal structures of **I-Vrd-NN** and **NN-Vrd-NN** were solved by X-ray crystallographic analysis. Monoradical precursor **I-Vrd-I** upon crystallization from various solvents gives tightly intertwined fine-needle crystals. The crystals were too thin, not suitable for single crystal X-ray study. ORTEP drawings with a numbering scheme of both paramagnets are

https://doi.org/10.1021/jacs.1c02938
J. Am. Chem. Soc. 2021, 143, 8164−8176

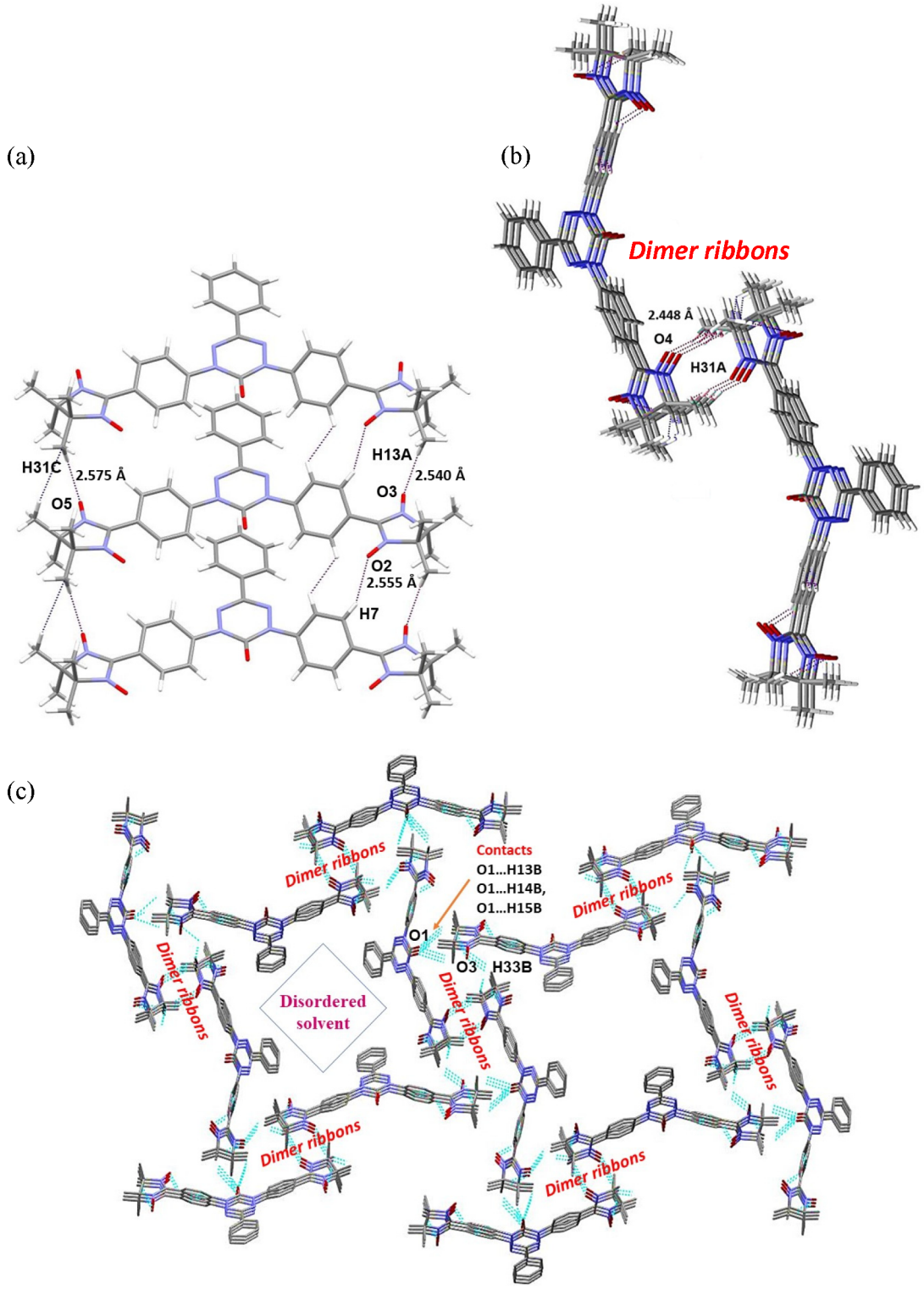

Figure 4. A fragment of the crystal structure showing a ribbon of **NN-Vrd-NN** triradicals (a), a dimer of ribbons (b), and their packing (c). Short intermolecular contacts, including those of nitroxide oxygens are indicated by dotted lines.

given in Figure 3a,b; the selected bond distances and angles with their estimated standard deviations are listed in Table S2.1.

In crystalline paramagnets **I-Vrd-NN** and **NN-Vrd-NN**, bond lengths in the NN and Vrd parts are close to the average values reported for these types of radicals.[43,44] The Vrd and phenyl rings are nearly planar. The imidazoline rings have a twisted shape (C_2 symmetry): in **I-Vrd-NN**, the C10 and C11 atoms are located on opposite sides of the plane of the NN moiety at distances of 0.145 and 0.195 Å, and in **NN-Vrd-NN**, atoms C10, C11, C29, and C30 are located at distances of 0.220−0.284 Å. The NN groups are twisted at different angles (28.3−51.3°) relative to the phenyl rings, as the phenyl rings are twisted in relation to the Vrd ring (6.9° and 11.5° for

https://doi.org/10.1021/jacs.1c02938
J. Am. Chem. Soc. 2021, 143, 8164−8176

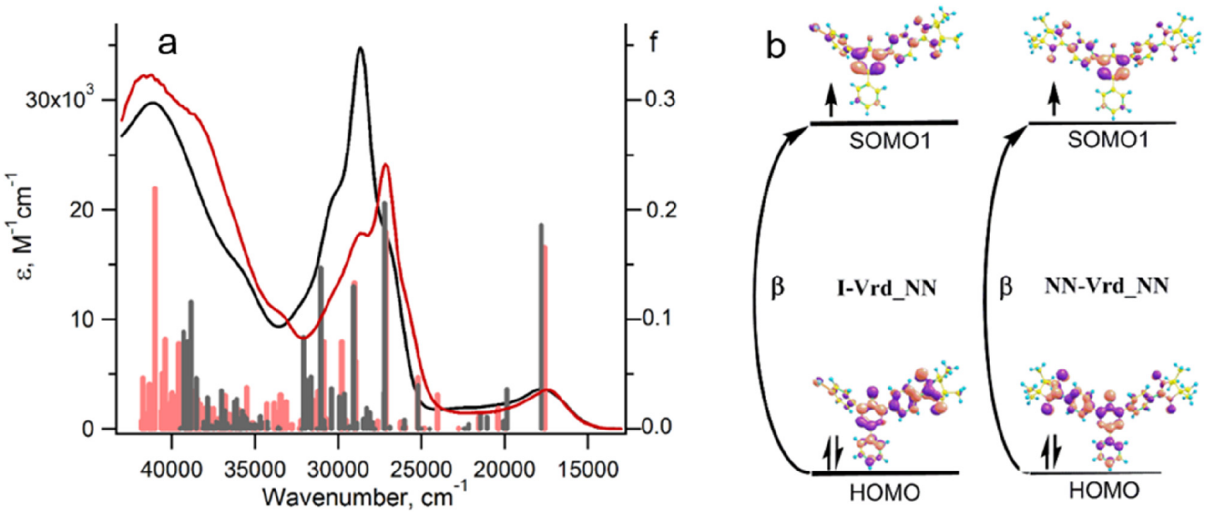

Figure 5. Experimental UV−vis spectra of the **I-Vrd-NN** diradical (red) and **NN-Vrd-NN** triradical (black). The vertical bars indicate positions and oscillator strengths (right axis) of the electronic transitions calculated at the TD-UB3LYP/def2-TZVP level for **I-Vrd-NN** (red bars) and **NN-Vrd-NN** (black bars) (a). The excitations (HOMO → SOMO1) that contribute mainly to the long-wavelength bands of the **I-Vrd-NN** diradical and **NN-Vrd-NN** triradical (b).

slightly twisted C22−C27 phenyl rings and from 22.40° to 53.2° for the other rings).

The **I-Vrd-NN** diradical crystallizes as a 1:1 solvate with acetone in the triclinic *P*-1 space group. The crystal packing of the diradical is characterized by short intermolecular contacts O3···H21 (2.533 Å) leading to the formation of centrosymmetrical dimers (Figure S2.1 and Table S2.2). Each dimer is linked with two adjacent dimers by short contacts O2···H18 (2.656 Å), thus yielding a ribbon structure. Acetone molecules fill the space between the ribbons occupying a fixed position due to numerous short contacts (such as O_{Ace}···H_{Me}, O_{Ace}···H_{Ph}, and H_{Ace}···O_{NO}) with diradical molecules and with neighboring acetone (Figure S2.2).

The **NN-Vrd-NN** triradical crystallizes in the tetragonal $P4_2/n$ space group where free volume is occupied by highly disordered solvent molecules. In the triradical's crystals, oxygen atoms of one nitroxide group form short intermolecular contacts O3···H13A (2.540 Å) and O2···H7 (2.555 Å) with hydrogen atoms of one of the methyl groups and phenyl moiety, respectively (Figure 4a, Table S2.2). Such contacts give rise to ribbons in which the oxygen atom of another nitroxide group forms the O5···H31C contact (2.575 Å). Rotation of the crystal structure of **NN-Vrd-NN** clearly demonstrated that the ribbon is connected by short O4···H31A contacts (2.448 Å) with the neighboring ribbon to form a centrosymmetric fragment (Figure 4b). Finally, the dimeric units are packed due to intermolecular short contacts with the participation of Vrd oxygen atoms O1···H13B, O1···H14B, and O1···H15B (2.487−2.700 Å) and nitroxide oxygen atoms O3···H33B (2.494 Å) with the formation of a parquet motif (Figure 4c). Another important feature of the crystal structure is the formation of infinite π-stacks between the Vrd and phenyl rings (C22−C27): The distances between the molecular planes inside the stacks are 3.55 Å [Cg···Cg 3.573(2) Å] for **I-Vrd-NN** and 3.54 Å [Cg···Cg 3.710(2) Å] for **NN-Vrd-NN** (Figure S2.4)

To study the electronic structure of the mono-, di-, and triradical, we used UV−vis spectroscopy, cyclic voltammetry, and theoretical methods for the interpretation of results. Analysis of the UV−vis spectra (Figure S3.1 and SI Section S3) showed that the long-wavelength bands of all the compounds have similar maxima (562−576 nm) and intensities. By contrast, the spectra revealed the sufficient differences in the 300−400 nm region (or 25,000−33,000 cm^{-1}): If we go from the Vrd radical **I-Vrd-I** to the di- and triradical (**I-Vrd-NN** and **NN-Vrd-NN**), the broad structureless band of the monoradical was replaced by a band characteristic of NN radicals with vibrational structure.[45] To assign the absorption bands and to understand similarities and differences between these spectra, we performed time-dependent DFT calculations at the TD-UB3LYP/def2-TZVP level of theory.

The calculations were in good agreement with experimental UV−vis spectra of **I-Vrd-NN** and **NN-Vrd-NN** (Figure 5a). The long-wavelength transitions in di- and triradicals mainly cause a redistribution of the electronic density within the Vrd moiety, similar to the case of the **I-Vrd-I** radical (Figure 5b and Figure S3.5).

According to the calculations, SOMO1 orbitals in all three compounds have similar energies and are localized mainly on Vrd moieties with minor delocalization to NN moieties. SOMO2 in **I-Vrd-NN** as well as SOMO2 and SOMO3 in **NN-Vrd-NN** are localized exclusively on NN moieties, and their energies are almost identical (Figure S3.6). The arrangement of the orbitals in the energy diagram and the corresponding distributions of the electron density are reflected in the electrochemical properties of paramagnets (Figure 6 and Table 1). The electrochemical properties of the synthesized di- and triradicals are consistent with the previous data obtained for the Vrd-NN diradicals.[26] Due to the proximity of the E^{ox} values for Vrd and NN moieties, we used the computational results (SI Section S3) to assign the electrochemical waves in di- and triradicals. Based on the known relationship[46] between E^{SOMO} and E^{ox} and that E^{SOMO}(NN) is higher than E^{SOMO}(Vrd), we concluded that E^{ox}(NN) is lower than E^{ox}(Vrd). Electrochemical reduction of the Vrd moiety in the mono-, di-, and triradicals in CH_2Cl_2 appears as one-electron reversible reduction waves with half-wave potentials of approximately −0.90 V (versus Fc/Fc^+, hereinafter). Likewise, the oxidation processes associated with the Vrd fragment are characterized by reversible or quasi-reversible waves with similar half-wave

https://doi.org/10.1021/jacs.1c02938
J. Am. Chem. Soc. 2021, 143, 8164−8176

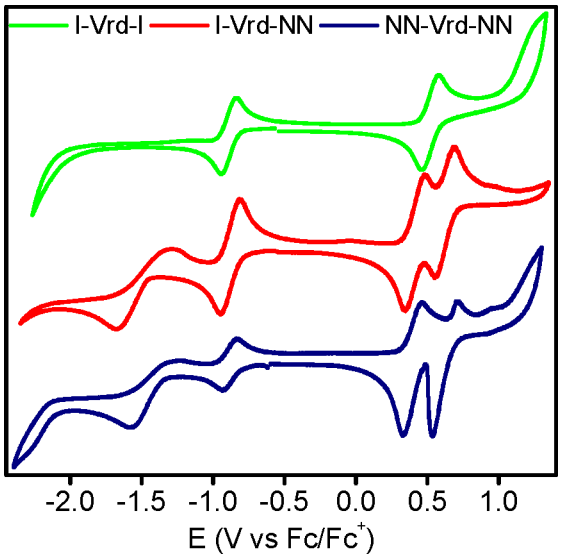

Figure 6. Cyclic voltammograms of the mono-, di-, and triradical in CH_2Cl_2 solution (100 mV/s with 0.1 M Bu_4NPF_6 as an electrolyte).

Table 1. Oxidation and Reduction Potentials of the Mono-, Di-, and Triradicals in CH_2Cl_2[a]

compound	$E^{1/2}_{Red2}$	$E^{1/2}_{Red1}$	$E^{1/2}_{Ox1}$	$E^{1/2}_{Ox2}$
I-Vrd-I	–	−0.89	–	0.52
NN-R[b]	−1.45	–	0.40	–
I-Vrd-NN	−1.48	−0.88	0.41	0.62
NN-Vrd-NN	−1.45[c]	−0.88	0.39[c]	0.61[c]

[a]Potentials are presented in V vs Fc/Fc^+. [b]Previously found potentials for NN-moiety in Vrd-NN diradicals.[26] [c]Quasi-reversible processes.

potentials: +0.52 V for **I-Vrd-I** and approximately +0.60 V for **I-Vrd-NN** and **NN-Vrd-NN**. The observed potentials are typical of radicals of the Vrd family.[47] The next set of redox waves (approximately −1.46 and +0.40 V) is associated with reduction and oxidation of the NN groups, respectively. It should be noted that the redox processes are reversible only in the **I-Vrd-NN** diradical and become quasi-reversible in the **NN-Vrd-NN** triradical.

Figure 7 shows continuous-wave (CW) EPR spectra of **I-Vrd-I**, **I-Vrd-NN**, and **NN-Vrd-NN** recorded in toluene solutions at room temperature. In this series, as the number of radical centers per molecule increases, the EPR spectrum becomes progressively narrower and less resolved due to a combination of verdazyl and NN moieties (Figure 7a).

The EPR spectrum of the **I-Vrd-I** monoradical can be well reproduced using four isotropic ^{14}N hyperfine interaction (HFI) constants A_1 = 0.644, A_2 = 0.633, A_3 = 0.454, and A_4 = 0.427 mT and g = 2.007 (Figure 7b). These parameters are in good agreement with the literature data on 6-oxoverdazyl radicals.[48]

For a simulation of the EPR spectrum of the **I-Vrd-NN** diradical, it is necessary to take into account six nitrogen nuclei with six HFI constants. Due to the significant exchange interaction between the two radical centers, each HFI constant must be halved. Thus, the EPR spectrum of **I-Vrd-NN** can be simulated by means of the constants A_1−A_4 obtained above, divided by 2, as well as the two HFI constants of the NN moiety (A_5 = 0.726 and A_6 = 0.722 mT), also divided by 2 (Figure 7c). The nitrogen atoms of the NN moiety are almost equivalent, and A_5 and A_6 are very close to the typical values for NN radicals.[49] The set of parameters "A_i = 0.322, 0.317, 0.227, 0.213, 0.363, 0.361 mT (for i = 1−6) and g = 2.008" leads to the best fit.

Similarly, the EPR spectrum of the **NN-Vrd-NN** triradical can be simulated taking into account eight nitrogen atoms (sum of Vrd and two of NN moieties) and their HFI constants divided by 3 owing to significant exchange interactions among three radical centers. The set of parameters "A_i = 0.215, 0.210, 0.153, 0.143, 0.243, 0.253, 0.249, 0.247 mT (for i = 1−8) and g = 2.0085" corresponds to the best fit (Figure 7d). Analysis of all best-fit parameters revealed perfect agreement of the experimental scaling factors with the expected values of 2 and 3 for the di- and triradical, respectively. This is convincing evidence that in liquid solutions synthesized derivatives **I-Vrd-NN** and **NN-Vrd-NN** are in the form of a di- and triradical, respectively, and intramolecular exchange interactions are strong (on the EPR scale). Auxiliary pulse EPR experiments in frozen solutions provided additional confirmations of these findings (SI Section S4).

Bulk magnetic properties of the **I-Vrd-I** radical, **I-Vrd-NN** diradical, and **NN-Vrd-NN** triradical were experimentally investigated by SQUID magnetometry of polycrystalline samples. In the case of the **I-Vrd-I** radical, χT vs T dependence is in excellent agreement with the Curie−Weiss law for molar magnetic susceptibility with negative Weiss temperature T_W = −4 K, indicating the weak antiferromagnetic (AF) exchange interactions between radicals. For the **I-Vrd-NN** diradical, the high-temperature value of χT is 0.94 $cm^3 \cdot K \cdot mol^{-1}$, which is between a theoretical one of 0.75 $cm^3 \cdot K \cdot mol^{-1}$ for two non-interacting spins S = 1/2 and 1.00 $cm^3 \cdot K \cdot mol^{-1}$ for one paramagnetic center with spin S = 1. With decreasing temperature, χT increases reaching 1.00 $cm^3 \cdot K \cdot mol^{-1}$ at 70 K and then decreases to 0.51 $cm^3 \cdot K \cdot mol^{-1}$ at 2 K (Figure 8a). The shape of the χT dependence on temperature for the sample of the **NN-Vrd-NN** triradical is similar to that of the diradical, except that it starts from a high-temperature value of 1.18 $cm^3 \cdot K \cdot mol^{-1}$, then reaches a maximum value of 1.31 $cm^3 \cdot K \cdot mol^{-1}$ at 50 K, and drops to 0.64 $cm^3 \cdot K \cdot mol^{-1}$ at 2 K. Therefore, at high temperatures, χT is close to the theoretical value of 1.125 $cm^3 \cdot K \cdot mol^{-1}$ for three non-interacting spins S = 1/2. Maximum χT value, 1.31 $cm^3 \cdot K \cdot mol^{-1}$, turned out to be much lower than the theoretical value 1.875 $cm^3 \cdot K \cdot mol^{-1}$ for S = 3/2 and close to 1.375 $cm^3 \cdot K \cdot mol^{-1}$ for non-interacting spins S_1 = 1 and S_2 = 1/2, which is the indication of one moderate ferromagnetic (FM) exchange interaction and two much weaker interactions. Our quantum chemical calculations confirm the significant difference in J_{ij} values. A decrease of the χT with lowering T below 50 K is most likely caused by the intermolecular AF interactions, although, in the general case, two weak intramolecular AF interactions can also lead to a decrease in χT to 0.375 $cm^3 \cdot K \cdot mol^{-1}$. To shed light on the origin of the observed magnetic behavior of the **I-Vrd-NN** diradical and **NN-Vrd-NN** triradical, intra- and intermolecular exchange interactions were analyzed theoretically using XRD crystal structures.

Prior to discussing the calculated values of J_{ij} parameters ($\hat{H} = -2\sum J_{ij}\hat{S}_i\hat{S}_j$), we briefly consider the electronic structure of **I-Vrd-NN** and **NN-Vrd-NN**. Figure S6.1 displays the nine active MOs of the CASSCF(9,10) calculations for the **I-Vrd-NN** diradical; the occupation numbers of two of these MOs are equal to 1 (1.0016 and 0.9999). Moreover, in both states, triplet and singlet, the configuration with four doubly occupied

https://doi.org/10.1021/jacs.1c02938
J. Am. Chem. Soc. 2021, 143, 8164−8176

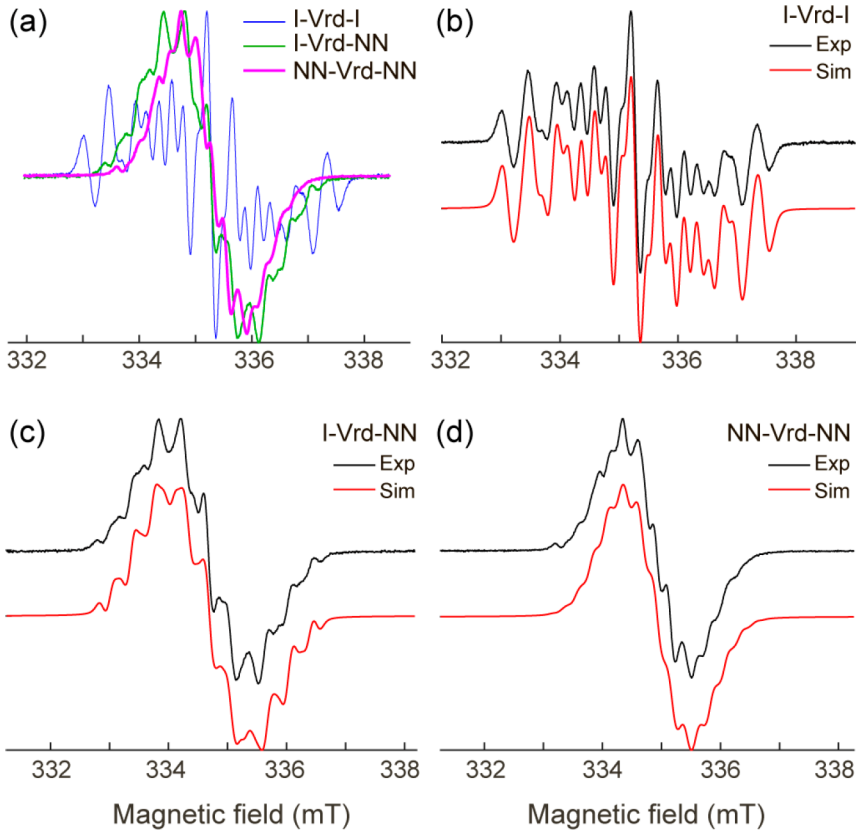

Figure 7. X-band room-temperature CW EPR spectra of **I-Vrd-I**, **I-Vrd-NN**, and **NN-Ver-NN** in the toluene solutions. (a) Experimental spectra of all the compounds. (b–d) Experimental (black) and simulated (red) spectra of the indicated compounds; parameters of the simulations are given in the text.

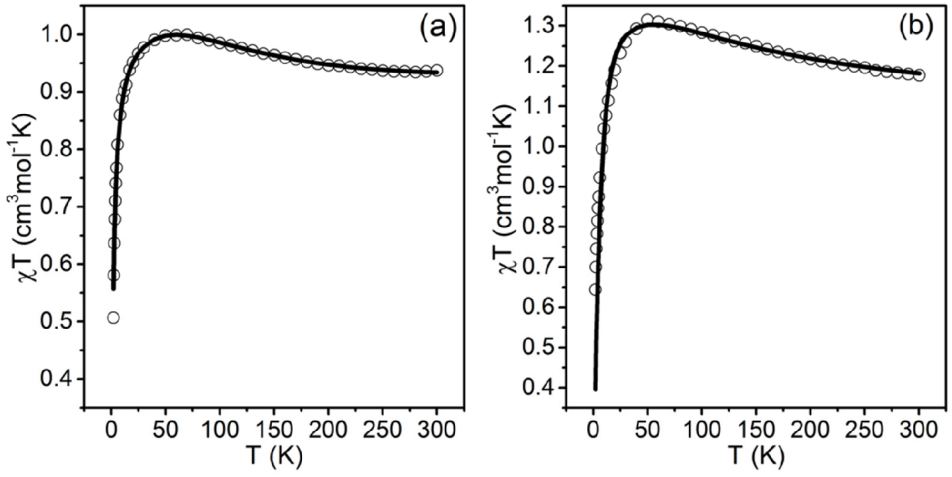

Figure 8. SQUID magnetometry of the polycrystalline samples of the **I-Vrd-NN** diradical (a) and the **NN-Vrd-NN** triradical (b): Plots of χT vs T at H = 5000 Oe in warming mode (open circles) and their best-fitting (solid curves) using magnetic models and parameters described in the text.

and two singly occupied MOs prevails (>83%). Thus, the **I-Vrd-NN** molecule has a purely diradical character in the lowest triplet and singlet states. The **NN-Vrd-NN** molecule has also a purely triradical character, since the occupation numbers of three of nine active MOs are equal to 1.000 (Figure S6.2).

To compute the parameters of intramolecular exchange interactions in **I-Vrd-NN** and **NN-Vrd-NN**, both the high-level CASSCF/NEVT2 and BS-UB3LYP calculations were performed. For the **I-Vrd-NN** diradical, CASSCF(9,10) (Figure S6.1) calculations predicted a moderate ferromagnetic interaction with singlet–triplet splitting $\Delta E_{ST}/k_B$ = 69.9 K (J/k_B = 35.0 K). The consideration of the dynamic electron correlation at the NEVPT2 level led to a 2-fold increase in $\Delta E_{ST}/k_B$ to 134.6 K (J_{dir}/k_B = 67.3 K). BS-DFT computations for the **I-Vrd-NN** diradical predicted the same sign of J, but a significantly higher absolute value of J/k_B = 283 K. The value of $\Delta E_{ST}/k_B = 2J/k_B$ = 566 K predicted at this level is much higher than ambient temperature (~300 K). It should be noted that such a phenomenon is similar to previous calculations for a series of Vrd-NN diradicals:[26] both procedures predict the

https://doi.org/10.1021/jacs.1c02938
J. Am. Chem. Soc. 2021, 143, 8164–8176

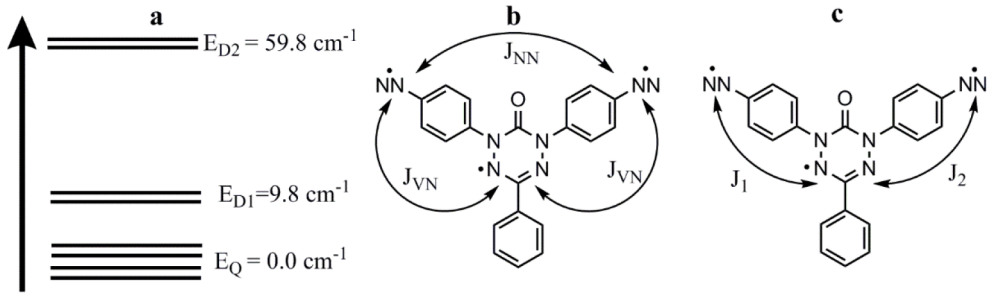

Figure 9. An energy diagram of the lowest-energy states of the **NN-Vrd-NN** triradical, as computed at the CASSCF(9,9)/CASPT2/def2-TZVP level of theory (a). Chemical structure of **NN-Vrd-NN** and proposed variants of exchange interactions between radical moieties described by two parameters (b and c).

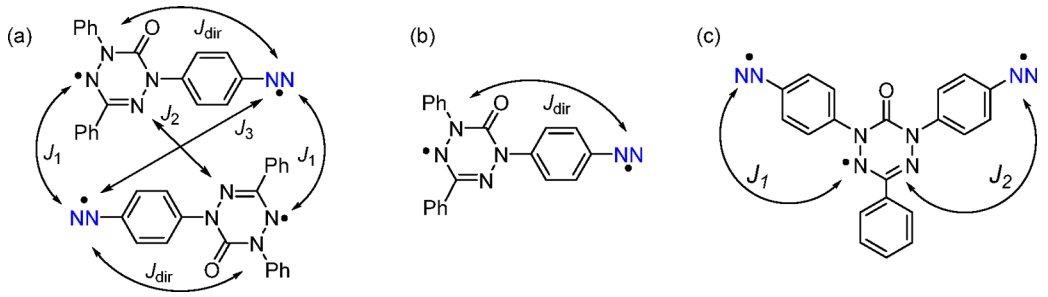

Figure 10. Magnetic motifs of **I-Vrd-NN** (a), simplified model (b), and **NN-Vrd-NN** (c).

same sign, but BS-DFT provides much higher absolute values of J.

For the **NN-Vrd-NN** triradical, CASSCF(9,9)/NEVPT2 (Figure S6.2) calculations predicted an energy splitting between the quartet ground state and two excited doublet states (Figure 9a). To determine the parameters of the exchange interactions between three radical moieties, the following assumptions should be made. If we assume a symmetrical geometry with two equivalent J_{VN} parameters (Figure 9b), then we obtain the following: J_{VN}/k_B = 28.2 K and J_{NN}/k_B = −7.3 K. If we ignore the interaction between the NN radical centers, then the remaining J_1/k_B and J_2/k_B values (Figure 9c) are estimated to be 38.8 and 10.1 K.

To select a more adequate interaction scheme (Figure 9b,c), we also performed calculations of three J parameters by the BS-DFT method. The exchange interaction between NN radical centers turned out to be negligibly small (J_{NN}/k_B = −0.3 K), whereas J_1/k_B and J_2/k_B were predicted to be 257 and 79 K, respectively. The difference between the J_1 and J_2 is related to different geometries of π-conjugated paths in the triradical: Although the Vrd and NN groups are practically coplanar (within ∼5°), the planes of phenylene linkers form different angles relative to this common plane (∼29° and ∼52°). Consequently, the model shown in Figure 9c adequately describes the important exchange interactions in the triradical, and the values of J_1/k_B = 38.8 and J_2/k_B = 10.1 K are their best theoretical estimates. Furthermore, BS-DFT calculations predict much higher (by approximately an order of magnitude) values of J_1 and J_2 in comparison to more accurate CASSCF/NEVPT2.

To assess intermolecular magnetic interactions, we first investigated intermolecular contacts with the participation of atoms having a relatively large spin density. For the di- and triradical, short contacts of the N−O···H_{Me} type and N−O···H_{Ph} type were identified at distances of 2.448 to 2.656 Å. In addition, **NN-Vrd-NN** crystals have short C═O···H_{Me} contacts of 2.487−2.700 Å. The magnetic interactions resulting from these contacts were calculated at the BS-B3LYP/def2-TZVP level via the conventional model of the nearest diradicals, in which H atoms are attached to remote radical centers. Parameters J/k_B of the intermolecular exchange interactions exceeding 2 K were predicted only for intradimer contacts in **I-Vrd-NN** (for details see SI Section S6). Parameters of these intradimer exchange interactions were also calculated at the CASSCF(10,10)/NEVPT2 level (Table S6.1).

Therefore, a magnetic motif of **I-Vrd-NN** crystals consists of isolated pairs of diradicals, the interactions between which can be accounted in the mean-field approximation (Figure 10a). This model is quite complicated and contains four paramagnetic centers and five parameters (J_{dir}, J_1, J_2, J_3, and zJ'). Attempts to use this model for simulation have demonstrated its overparametrization (for details see SI, Section S5). Thus, we used for the simulation simplified model of isolated diradicals (Figure 10b) in the mean field approximation (Figure 8a), which gives the following best-fit parameters: J_{dir}/k_B = 97 ± 7 K and zJ'/k_B = −2.5 ± 0.3 K. Note that the most accurate calculations predict J_{dir}/k_B = 67.3 K, which is in good agreement with experiment.

As for the **NN-Vrd-NN** triradical, the magnetic motif represents isolated paramagnetic species (a triradical with two ferromagnetic interactions, Figure 10c); the intermolecular interactions can be described in the mean field approximation (see for details SI, Section S5). The best agreement with experiment was achieved with the following parameters: J_1/k_B = 105 ± 16 K, J_2/k_B = 17 ± 2 K, and zJ'/k_B = −5.6 ± 0.2 K (Figure 8b). These J_1 and J_2 values correspond to the following energies of the doublet states: E_{D1} = 17 cm^{-1} and E_{D2} = 152 cm^{-1}. It is worth mentioning that the most accurate theoretical predictions are 9.8 and 59.8 cm^{-1}, respectively (Figure 9), which are in fair agreement with the experimental estimates.

https://doi.org/10.1021/jacs.1c02938
J. Am. Chem. Soc. 2021, 143, 8164−8176

CONCLUSION

In this work, we succeeded in preparing a heterospin triradical containing oxoverdazyl and two NN moieties. The triradical has bridging units of the ethylene-1,1-diyl type and, therefore, a quartet ground state. The triradical is stable in air and possesses good thermal stability in an inert atmosphere. The Vrd and NN centers showed reversible (at −0.88 and 0.41 V vs Fc/Fc^+) and quasi-reversible (at −1.48 and ∼0.61 V vs Fc/Fc^+, in CH_2Cl_2) redox waves. The magnetic properties were characterized by SQUID magnetometry of polycrystalline powders and by EPR spectroscopy in various matrices and analyzed with reference to XRD data and high-level quantum chemical calculations. The results point to rather strong intramolecular ferromagnetic exchange interactions. The obtained heterospin triradical with quartet ground state can be further functionalized which opens possibility for design and synthesis of stable polyradicals with very high-spin ground state for the development of purely organic magnetic and electronic materials.

EXPERIMENTAL SECTION

General Procedures. DMF was dried and distilled over calcium hydride. Other solvents were of reagent quality. All organic reagents and solvents were purchased from commercial suppliers (Sigma-Aldrich, Alfa Aesar, and others) and were used as received. Nitronyl nitroxide-2-ide gold(I) complex (Ph_3P-Au-NN) was prepared according to a previously reported procedure.[39] All reactions were carried out under argon in oven-dried Schlenk flasks. Routine monitoring of the reactions was performed by means of silica-coated aluminum plates (Merck, Silica gel 60, F254), which were analyzed under UV light at 254 nm. Chromatography was carried out on silica (0.050−0.160 mm) for column chromatography.

IR spectra were recorded with a Bruker Tensor 27 FTIR spectrometer in KBr pellets. UV−vis spectra were acquired in a CH_2Cl_2 solution on a Bruker Vector-22 spectrometer. Melting points were determined by means of an FP 900 Thermosystem microscope melting point apparatus (Mettler-Toledo International Inc., Zürich, Switzerland), and elemental analysis was performed on a Carlo Erba CHN analyzer.

Cyclic voltammetry measurements were performed at a sweep rate of 0.1 $V{\cdot}s^{-1}$ in a deoxygenated CH_2Cl_2 solution by a computer-controlled P-8 nano potentiostat/galvanostat (Elins, Russia) in combination with a three-electrode cell (Gamry), with 0.1 M Bu_4NPF_6 as a supporting electrolyte. Pt, a Pt wire, and Ag/AgCl served as working, counter, and reference electrodes, respectively. The reference electrode was calibrated by measurement of the redox potentials of ferrocene. The redox event centered at 0 mV corresponds to the ferrocene/ferrocenium redox couple (ferrocene added as an internal reference).

All EPR data were collected using X/Q-band pulse/cw EPR spectrometer Bruker Elexsys E580 equipped with an Oxford Instruments temperature control system (T = 4−300 K). For all spectral simulations, the EasySpin toolbox for Matlab was utilized.[50]

The magnetic susceptibility of the polycrystalline samples was measured with a Quantum Design MPMS*XL* SQUID magnetometer in the temperature range of 2−300 K with a magnetic field of up to 5 kOe. None of complexes exhibited any field dependence of molar magnetic susceptibility at low temperatures. Diamagnetic corrections were made using the Pascal constants.[51] The spin Hamiltonian in general form of $\hat{H} = -2J\hat{S}_1\hat{S}_2$ was used for an analysis of the experimental χT(T) dependencies.

Synthesis of Diiodoverdazyl Radical I-Vrd-I, Diradical I-Vrd-NN, and Triradical NN-Vrd-NN. Standard techniques for synthesis in an argon atmosphere were used, including Schlenk glassware and manifold high-vacuum lines. The multistep, efficient synthesis and characterization of starting diiodoverdazyl building block **I-Vrd-I** are outlined in Scheme S1.

*Synthesis of Diradical **I-Vrd-NN** and Triradical **NN-Vrd-NN**.* Verdazyl iodide **I-Vrd-I**, Ph_3P-Au-NN, and $Pd(PPh_3)_4$ were dissolved in DMF under argon (amounts of the reagents are given in Table 2).

Table 2. Yields of I-Vrd-NN and NN-Vrd-NN Depending on the Reagent Ratio and Reaction Time

					yields (%)	
entry	**I-Vrd-I** (mmol)	Ph_3P-Au-NN (mmol)	$Pd(PPh_3)_4$ (% mol)	time (h)	**I-Vrd-NN**	**NN-Vrd-NN**
1	0.135	0.202	10	1.5	34	27
2	0.4211	0.6318	10	1.5	20	3
3	0.0863	0.259	20	3	27	14

The mixture was heated at 70 °C until full conversion of the starting Au complex (monitored by TLC in dichloromethane-EtOAc at 35:1). Then, the reaction mixture was cooled to room temperature, and the solvent was removed in vacuo. Products **I-Vrd-NN** and **NN-Vrd-NN** were isolated by column chromatography (SiO_2, from EtOAc-hexane at 1:3 to EtOAc-hexane at 1:1 to EtOAc alone) and next crystallized from an acetone-heptane solution.

*1-(4-(4,4,5,5-Tetramethyl-3-oxide-1-oxyl-4,5-dihydro-1H-imidazol-2-yl)phenyl)-3-(4-iodophenyl)-5-phenyl-2-oxoverdazyl diradical (**I-Vrd-NN**).*

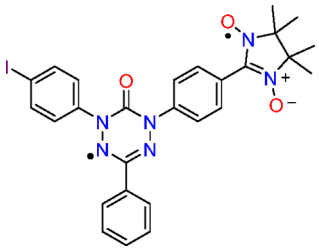

Dark purple powder. Mp (5 °C/min): 129.7 °C (decomp.). UV (CH_2Cl_2) λ_{max} (lg ε): 574 (3.49), 368 (4.36), 350 (4.25), 242 (4.50) nm. IR (KBr, cm^{-1}): 3439, 3398, 3090, 3064, 3036, 2987, 2949, 2926, 2868, 2854, 1761, 1703, 1599, 1581, 1522, 1481, 1450, 1414, 1390, 1365, 1311, 1279, 1248, 1217, 1167, 1124, 1101, 1061, 1041, 1022, 1005, 970, 895, 868, 837, 825, 806, 773, 712, 694, 656, 634, 619, 542, 527, 509, 451. High-resolution mass spectrometry (HRMS; ESI-QTOF) calcd for $C_{27}H_{25}IN_6O_3$ [M^-]: 608.1033. Found: 608.1039. Anal. calcd for $C_{27}H_{25}IN_6O_3{\cdot}$acetone: C, 54.06; H, 4.69; N, 12.61. Found: C, 54.11; H, 4.64; N, 12.57.

*1,3-(4-(4,4,5,5-Tetramethyl-3-oxide-1-oxyl-4,5-dihydro-1H-imidazol-2-yl)phenyl)-5-phenyl-2-oxoverdazyl triradical (**NN-Vrd-NN**).*

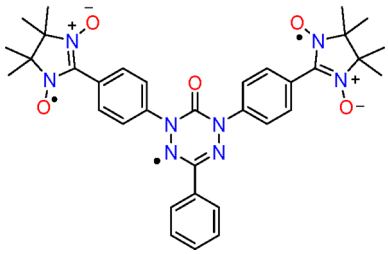

Dark purple powder. Mp (1 °C/min): 133.6 °C (decomp.). UV (CH_2Cl_2) λ_{max}, (lg ε): 583 (3.56), 369 (4.55), 263 (4.48) nm. FT-IR (KBr, cm^{-1}): 3437, 3091, 3057, 2987, 2937, 2872, 1705, 1599, 1520, 1483, 1468, 1450, 1435, 1421, 1412, 1389, 1365, 1311, 1248, 1217, 1190, 1167, 1134, 1101, 1074, 1043, 1018, 968, 868, 839, 773, 760, 721, 694, 656, 634, 619, 542, 527, 446. HRMS (ESI-QTOF) calcd for $C_{34}H_{37}N_8O_5$ [M^-]: 637.2887. Found: 637.2878. Anal. calcd for $C_{34}H_{37}N_8O_5{\cdot}$acetone: C, 63.87; H, 6.23; N, 16.10. Found: C, 63.71; H, 6.25; N, 16.13.

X-ray Crystallography. Crystals of **I-Vrd-NN** and **NN-Vrd-NN** for this analysis were prepared by slow evaporation from a solution in

https://doi.org/10.1021/jacs.1c02938
J. Am. Chem. Soc. 2021, 143, 8164−8176

acetone-heptane at 5 °C. Data collection was performed on a Bruker Kappa Apex II CCD diffractometer using φ,ω-scans of narrow (0.5°) frames with Mo Kα radiation (λ = 0.71073 Å) and a graphite monochromator. The structures were solved by direct methods in the SHELX-97 software[52] and were refined by the full-matrix least-squares method over all F^2 in anisotropic approximation using the SHELXL-2014/7 software.[53] Absorption corrections were made by an empirical multiscan method with the SADABS program.[54] Hydrogen atom positions were calculated with the riding model. The crystallographic data are listed in Table 3.

Table 3. XRD Data for Compounds I-Vrd-NN and NN-Vrd-NN

compound	I-Vrd-NN	NN-Vrd-NN
empirical formula	$C_{27}H_{25}N_6O_3I{\cdot}C_3H_6O$	$C_{34}H_{37}N_8O_5{\cdot}$solvent
formula weight	666.51	637.71
temperature (K)	200(2)	200(2)
wavelength (Å)	0.71073	0.71073
crystal system	triclinic	tetragonal
space group	*P*-1	$P4_2/n$
unit cell dimensions *a* (Å)	10.8641(6)	35.3952(18)
b (Å)	11.4045(5)	35.3952(18)
c (Å)	12.9351(7)	6.2920(4)
α (°)	85.947(2)	90
β (°)	85.585(2)	90
γ (°)	66.789(2)	90
volume (Å^3)	1467.1(1)	7882.7(9)
Z	2	8
density (calcd) (mg·m^{-3})	1.509	1.075
abs. coefficient (mm^{-1})	1.137	0.074
F(000)	676	2696
crystal size (mm^3)	0.04 × 0.20 × 0.90	0.04 × 0.08 × 0.90
Θ range for data collection (°)	2.04−30.07	1.15−26.12
	$-15 \le h \le 15$	$-43 \le h \le 43$
index ranges	$-16 \le k \le 13$	$-43 \le k \le 43$
	$-18 \le l \le 16$	$-7 \le l \le 7$
reflections collected	31551	91377
independent reflections	7843 *R*(int) = 0.034	7820 *R*(int)= 0.125
completeness to θ (%)	99.9	99.9
data/restraints/parameters	7843/0/376	7820/0/432
goodness-of-fit on F^2	1.005	1.03
final *R* indices $I > 2\sigma(I)$	R_1 = 0.0375, wR_2 = 0.0951	R_1 = 0.0619, wR_2 = 0.1298
final *R* indices (all data)	R_1 = 0.0606, wR_2 = 0.1096	R_1 = 0.1345, wR_2 = 0.1561
largest diff. peak/hole (e·Å^{-3})	1.01/−0.56	0.26/−0.21
CCDC	2068922	2068923

The obtained crystal structures were analyzed for short contacts between nonbonded atoms using PLATON[55,56] and MERCURY programs.[57] The crystal structure of **I-Vrd-NN** is formed by one solvating molecule of acetone per unit. The free volume accessible to the solvent in the **NN-Vrd-NN** crystal derived from the PLATON[54] routine analysis is 19% (1504 Å^3). This volume is occupied by highly disordered solvent molecules, which could not be modeled as a set of discrete atomic sites. We employed the PLATON/SQUEEZE procedure to calculate the diffraction contribution from the solvent region and thereby produced a set of solvent-free diffraction intensities. The most probable solvate molecule for **NN-Vrd-NN** is acetone.

CCDC 2068922 and 2068923 contain the supplementary crystallographic data for this paper. These data can be obtained free of charge via https://www.ccdc.cam.ac.uk/, or from the Cambridge Crystallographic Data Centre, 12 Union Road, Cambridge CB2 1EZ, UK; fax: (+44) 1223 336 033; or e-mail: deposit@ccdc.cam.ac.uk.

Computational Details. For the **I-Vrd-I** radical, all calculations were performed for the geometry optimized at the UB3LYP/def2-TZVP level.[58−60] For the **I-Vrd-NN** diradical and **NN-Vrd-NN** triradical, the calculations were mainly performed for XRD structures. Electronic absorption spectra (UV−vis spectra) of the paramagnetic compounds were computed via time-dependent DFT calculations[61] with the B3LYP functional[58,59] and the def2-TZVP basis set.[60] In the case of the **I-Vrd-NN** diradical and **NN-Vrd-NN** triradical, the UV−vis spectra were calculated for their high-spin ground states (a triplet state for **I-Vrd-NN** and a quartet state for **NN-Vrd-NN**).

The parameters of the intramolecular exchange interactions (J) were computed for pairs of paramagnetic centers ($\hat{H} = -2J\hat{S}_1\hat{S}_2$) by two procedures. The accurate ab initio CASSCF[62] and CASSCF/NEVPT2.[63,64] procedures were mainly employed. The spin-unrestricted broken-symmetry (BS) approach[65] was utilized too. The energies of the high-spin states (E^{HS}) and low-spin states within the BS approach (E^{LS}_{BS}) were calculated at the UB3LYP level of theory, and the J values were computed according to the following formula:[66]

$$J = \frac{E^{HS} - E^{LS}_{BS}}{\langle S^2\rangle^{HS} - \langle S^2\rangle^{LS}_{BS}}$$

Parameters of the intermolecular exchange interactions (J) were calculated mainly at the BS-UB3LYP/def2-TZVP level. These values were calculated only for pairs of model radicals. To obtain model radicals, hydrogen atoms were added to remote radical centers of the di- and triradical. All the calculations were performed using the ORCA 4.0.1 software suite.[67]

■ ASSOCIATED CONTENT

Supporting Information

The Supporting Information is available free of charge at https://pubs.acs.org/doi/10.1021/jacs.1c02938.

Additional synthetic details, SQUID, XRD, ESR data, computation details and NMR and FTIR spectra (PDF)

Accession Codes

CCDC 2068922−2068923 contain the supplementary crystallographic data for this paper. These data can be obtained free of charge via www.ccdc.cam.ac.uk/data_request/cif, or by emailing data_request@ccdc.cam.ac.uk, or by contacting The Cambridge Crystallographic Data Centre, 12 Union Road, Cambridge CB2 1EZ, UK; fax: +44 1223 336033.

■ AUTHOR INFORMATION

Corresponding Authors

Evgeny V. Tretyakov − *N.D. Zelinsky Institute of Organic Chemistry, Russian Academy of Sciences, Moscow 119991, Russian Federation*; Email: tretyakov@ioc.ac.ru

Pavel V. Petunin − *Tomsk Polytechnic University, Tomsk 634050, Russian Federation*; orcid.org/0000-0001-7101-5996; Email: petuninpavel@tpu.ru

Victor I. Ovcharenko − *International Tomography Center, Siberian Branch of Russian Academy of Sciences, Novosibirsk 630090, Russian Federation*; Email: ovchar@tomo.nsc.ru

Nina P. Gritsan − *V.V. Voevodsky Institute of Chemical Kinetics and Combustion, Siberian Branch of Russian Academy of Sciences, Novosibirsk 630090, Russian Federation*; orcid.org/0000-0002-2263-1300; Email: gritsan@kinetics.nsc.ru

Authors

Svetlana I. Zhivetyeva − *N.N. Vorozhtsov Novosibirsk Institute of Organic Chemistry, Siberian Branch of Russian*

https://doi.org/10.1021/jacs.1c02938
J. Am. Chem. Soc. 2021, 143, 8164−8176

Academy of Sciences, Novosibirsk 630090, Russian Federation

Dmitry E. Gorbunov − *V.V. Voevodsky Institute of Chemical Kinetics and Combustion, Siberian Branch of Russian Academy of Sciences, Novosibirsk 630090, Russian Federation*

Matvey V. Fedin − *International Tomography Center, Siberian Branch of Russian Academy of Sciences, Novosibirsk 630090, Russian Federation;* orcid.org/0000-0002-0537-5755

Dmitri V. Stass − *V.V. Voevodsky Institute of Chemical Kinetics and Combustion, Siberian Branch of Russian Academy of Sciences, Novosibirsk 630090, Russian Federation; Novosibirsk State University, Novosibirsk 630090, Russian Federation*

Rimma I. Samoilova − *V.V. Voevodsky Institute of Chemical Kinetics and Combustion, Siberian Branch of Russian Academy of Sciences, Novosibirsk 630090, Russian Federation*

Irina Yu. Bagryanskaya − *N.N. Vorozhtsov Novosibirsk Institute of Organic Chemistry, Siberian Branch of Russian Academy of Sciences, Novosibirsk 630090, Russian Federation*

Inna K. Shundrina − *N.N. Vorozhtsov Novosibirsk Institute of Organic Chemistry, Siberian Branch of Russian Academy of Sciences, Novosibirsk 630090, Russian Federation*

Artem S. Bogomyakov − *International Tomography Center, Siberian Branch of Russian Academy of Sciences, Novosibirsk 630090, Russian Federation;* orcid.org/0000-0002-6918-5459

Maxim S. Kazantsev − *N.N. Vorozhtsov Novosibirsk Institute of Organic Chemistry, Siberian Branch of Russian Academy of Sciences, Novosibirsk 630090, Russian Federation;* orcid.org/0000-0002-2869-1777

Pavel S. Postnikov − *Tomsk Polytechnic University, Tomsk 634050, Russian Federation;* orcid.org/0000-0001-9713-1290

Marina E. Trusova − *Tomsk Polytechnic University, Tomsk 634050, Russian Federation*

Complete contact information is available at: https://pubs.acs.org/10.1021/jacs.1c02938

Notes

The authors declare no competing financial interest.

■ ACKNOWLEDGMENTS

This research was supported by the Russian Science Foundation (project no. 20-73-00236). The authors would like to acknowledge the Multi-Access Chemical Research Center SB RAS for spectral and analytical measurements. The authors thank Dr. Alexander Maryasov (Novosibirsk Institute of Organic Chemistry) for a fruitful discussion and useful comments. The authors would like to acknowledge the Research Resource Center "Irkutsk Supercomputer Center SB RAS" for the computational resources.

■ DEDICATION

In memory of Professor Keiji Okada.

■ REFERENCES

(1) *π-Electron Magnetism*; Veciana, J., Arčon, D., Deumal, M., Inoue, K., Kinoshita, M., Novoa, J. J., Palacio, F., Prassides, K., Rawson, J. M., Rovira, C., Eds.; Springer: Berlin, Heidelberg, 2001; Vol. *100*, Structure and Bonding series. DOI: 10.1007/3-540-44684-2

(2) Gatteschi, D.; Sessoli, R.; Villain, J. *Molecular Nanomagnets*; Oxford University Press: Oxford, 2006. DOI: 10.1093/acprof:oso/9780198567530.001.0001.

(3) Abe, M. Diradicals. *Chem. Rev.* **2013**, *113* (9), 7011−7088.

(4) Nishinaga, T. *Organic Redox Systems: Synthesis, Properties, and Applications*; Nishinaga, T., Ed.; John Wiley & Sons, Inc: Hoboken, NJ, 2015; pp 269 − 285. DOI: 10.1002/9781118858981.

(5) Baumgarten, M. High Spin Organic Molecules. *Mater. Energy* **2018**, *4*, 1−93.

(6) Sanvito, S. Molecular Spintronics. *Chem. Soc. Rev.* **2011**, *40* (6), 3336−3355.

(7) Hu, G.; Xie, S.; Wang, C.; Timm, C. Spin-Dependent Transport and Functional Design in Organic Ferromagnetic Devices. *Beilstein J. Nanotechnol.* **2017**, *8* (1), 1919−1931.

(8) Gaudenzi, R.; Burzurí, E.; Reta, D.; Moreira, I. D. P. R.; Bromley, S. T.; Rovira, C.; Veciana, J.; Van Der Zant, H. S. J. Exchange Coupling Inversion in a High-Spin Organic Triradical Molecule. *Nano Lett.* **2016**, *16* (3), 2066−2071.

(9) Akasaka, T.; Osuka, A.; Fukuzumi, S.; Kandori, H.; Aso, Y. *Chemical Science of π-Electron Systems*; Akasaka, T., Osuka, A., Fukuzumi, S., Kandori, H., Aso, Y., Eds.; Springer Japan: Tokyo, 2015; Vol. *8*. DOI: 10.1007/978-4-431-55357-1.

(10) Sugisaki, K.; Nakazawa, S.; Toyota, K.; Sato, K.; Shiomi, D.; Takui, T. Quantum Chemistry on Quantum Computers: A Method for Preparation of Multiconfigurational Wave Functions on Quantum Computers without Performing Post-Hartree-Fock Calculations. *ACS Cent. Sci.* **2019**, *5* (1), 167−175.

(11) Longuet-Higgins, H. C. Some Studies in Molecular Orbital Theory. I. Resonance Structures and Molecular Orbitals in Unsaturated Hydrocarbons. *J. Chem. Phys.* **1950**, *18* (3), 265−274.

(12) Borden, W. T.; Davidson, E. R. Effects of Electron Repulsion in Conjugated Hydrocarbon Diradicals. *J. Am. Chem. Soc.* **1977**, *99* (14), 4587−4594.

(13) Rajca, A.; Utamapanya, S. Poly(Arylmethyl) Quartet Triradicals and Quintet Tetraradicals. *J. Am. Chem. Soc.* **1993**, *115* (6), 2396−2401.

(14) Rajca, A.; Wongsriratanakul, J.; Rajca, S. Organic Spin Clusters: Ferromagnetin Spin Coupling through a Biphenyl Unit in Polyarylmethyl Tri-, Penta-, Hepta-, and Hexadecaradicals. *J. Am. Chem. Soc.* **1997**, *119* (48), 11674−11686.

(15) Gallagher, N. M.; Olankitwanit, A.; Rajca, A. High-Spin Organic Molecules. *J. Org. Chem.* **2015**, *80* (3), 1291−1298.

(16) Ovchinnikov, A. A. Multiplicity of the Ground State of Large Alternant Organic Molecules with Conjugated Bonds - (Do Organic Ferromagnetics Exist?). *Theor. Chim. Acta* **1978**, *47* (4), 297−304.

(17) Klein, D. J.; Nelin, C. J.; Alexander, S.; Matsen, F. A. High-Spin Hydrocarbons. *J. Chem. Phys.* **1982**, *77* (6), 3101−3108.

(18) Inoue, K.; Iwamura, H. 2-[p(N-tert-butyl-N-oxyamino)-Phenyl]-4,4,5,5-tetramethyl-4,5-dihydroimidazol-3-oxide-1-oxyl, a Stable Diradical with a Triplet Ground State. *Angew. Chem., Int. Ed. Engl.* **1995**, *34* (8), 927−928.

(19) Tanaka, M.; Matsuda, K.; Itoh, T.; Iwamura, H. Syntheses and Magnetic Properties of Stable Organic Triradicals with Quartet Ground States Consisting of Different Nitroxide Radicals. *J. Am. Chem. Soc.* **1998**, *120* (29), 7168−7173.

(20) Suzuki, S.; Furui, T.; Kuratsu, M.; Kozaki, M.; Shiomi, D.; Sato, K.; Takui, T.; Okada, K. Nitroxide-Substituted Nitronyl Nitroxide and Iminonitroxide. *J. Am. Chem. Soc.* **2010**, *132* (45), 15908−15910.

(21) Tretyakov, E. V.; Tolstikov, S. E.; Romanenko, G. V.; Bogomyakov, A. S.; Stass, D. V.; Maryasov, A. G.; Gritsan, N. P.; Ovcharenko, V. I. Method for the Synthesis of a Stable Heteroatom Analog of Trimethylenemethane. *Russ. Chem. Bull.* **2011**, *60* (12), 2608−2612.

(22) Rajca, A.; Olankitwanit, A.; Rajca, S. Triplet Ground State Derivative of Aza- m -Xylylene Diradical with Large Singlet-Triplet Energy Gap. *J. Am. Chem. Soc.* **2011**, *133* (13), 4750−4753.

(23) Gallagher, N. M.; Bauer, J. J.; Pink, M.; Rajca, S.; Rajca, A. High-Spin Organic Diradical with Robust Stability. *J. Am. Chem. Soc.* **2016**, *138* (30), 9377−9380.
(24) Wang, W.; Chen, C.; Shu, C.; Rajca, S.; Wang, X.; Rajca, A. S = 1 Tetraazacyclophane Diradical Dication with Robust Stability: A Case of Low-Temperature One-Dimensional Antiferromagnetic Chain. *J. Am. Chem. Soc.* **2018**, *140* (25), 7820−7826.
(25) Gallagher, N.; Zhang, H.; Junghoefer, T.; Giangrisostomi, E.; Ovsyannikov, R.; Pink, M.; Rajca, S.; Casu, M. B.; Rajca, A. Thermally and Magnetically Robust Triplet Ground State Diradical. *J. Am. Chem. Soc.* **2019**, *141*, 4764−4774.
(26) Tretyakov, E. V.; Zhivetyeva, S. I.; Petunin, P. V.; Gorbunov, D. E.; Gritsan, N. P.; Bagryanskaya, I. Y.; Bogomyakov, A. S.; Postnikov, P. S.; Kazantsev, M. S.; Trusova, M. E.; Shundrina, I. K.; Zaytseva, E. V.; Parkhomenko, D. A.; Bagryanskaya, E. G.; Ovcharenko, V. I. Ferromagnetically Coupled S = 1 Chains in Crystals of Verdazyl-Nitronyl Nitroxide Diradicals. *Angew. Chem., Int. Ed.* **2020**, *59* (46), 20704−20710.
(27) Veciana, J.; Rovira, C.; Ventosa, N.; Crespo, M. I.; Palacio, F. Stable Polyradicals with High-Spin Ground States. 2. Synthesis and Characterization of a Complete Series of Polyradicals Derived from 2,4,6-Trichloro-$\alpha,\alpha,\alpha',\alpha',\alpha'',\alpha''$-Hexakis(Pentachlorophenyl)-Mesitylene with S = 1/2, 1, and 3/2 Ground States. *J. Am. Chem. Soc.* **1993**, *115* (1), 57−64.
(28) Kothe, G.; Neugebauer, F. A.; Zimmermann, H. 1,3,5-Benzenetriyltris(1,5-diphenyl-3-verdazyl): A Radical Having a Nearly Degenerate Doublet-Quartet Ground State. *Angew. Chem., Int. Ed. Engl.* **1972**, *11*, 830−832.
(29) Rey, P.; Ovcharenko, V. I. Copper(II) Nitroxide Molecular Spin-Transition Complexes. In *Magnetism: Molecules to Materials*; Wiley-VCH: Weinheim, 2003; Vol. *4*−*5*, pp 41−63. DOI: 10.1002/9783527620548.ch2c.
(30) Iwamura, H.; Inoue, K. Magnetic Ordering in Metal Coordination Complexes with Aminoxyl Radicals. In *Magnetism: Molecules to Materials*; Wiley-VCH: Weinheim, 2003; Vol. *2*−*5*. DOI: 10.1002/9783527620548.ch2a.
(31) Dulog, L.; Kim, J. S. A Stable Triradical Compound and Its Unusual Magnetic Properties. *Angew. Chem., Int. Ed. Engl.* **1990**, *29* (4), 415−417.
(32) Izuoka, A.; Fukada, M.; Sugawara, T. Stable Mono-, Di-, and Triradicals as Constituent Molecules for Organic Ferrimagnets. *Mol. Cryst. Liq. Cryst. Sci. Technol., Sect. A* **1993**, *232* (1), 103−108.
(33) Izuoka, A.; Fukada, M.; Sugawara, T.; Sakai, M.; Bandow, S. Magnetic Property of 1,3,5-Tris(4′,4′,5′,5′-Tetramethylimidazolin-2′-Yl)Benzene 3′,3″,3‴-Trioxide 1′,1′′,1′′′-Trioxyl in 1:1 Mixed Crystals with 1,3,5-Trinitrobenzene. *Chem. Lett.* **1992**, *21* (8), 1627−1630.
(34) Izuoka, A.; Fukada, M.; Kumai, R.; Itakura, M.; Hikami, S.; Sugawara, T. Magnetically Coupled Molecular System Composed of Organic Radicals with Different Spin Multiplicities. *J. Am. Chem. Soc.* **1994**, *116* (6), 2609−2610.
(35) Kanno, F.; Inoue, K.; Koga, N.; Iwamura, H. Persistent 1,3,5-Benzenetriyltris(*N-Tert*-Butyl Nitroxide) and Its Analogs with Quartet Ground States. Intramolecular Triangular Exchange Coupling among Three Nitroxide Radical Centers. *J. Phys. Chem.* **1993**, *97* (50), 13267−13272.
(36) Hayami, S.; Inoue, K. Structure and Magnetic Property of the Organic Triradical with Triazine Skeleton; 2,4,6-Tris{p-(N-Oxy-N-Tert-Butylamino)Phenyl}triazine. *Chem. Lett.* **1999**, *28* (7), 545−546.
(37) Lahti, P. M.; Liao, Y.; Julier, M.; Palacio, F. S-Triazine As an Exchange Linker in Organic High-Spin Molecules. *Synth. Met.* **2001**, *122* (3), 485−493.
(38) Ishida, T.; Iwamura, H. Bis[3-Tert-Butyl-5-(*N*-Oxy-*Tert*-Butylamino)Phenyl] Nitroxide in a Quartet Ground State: A Prototype for Persistent High-Spin Poly [(Oxyimino)-1,3-Phenylenes]. *J. Am. Chem. Soc.* **1991**, *113* (11), 4238−4241.
(39) Trindle, C.; Datta, S. N.; Mallik, B. Phenylene Coupling of Methylene Sites. The Spin States of Bis(x- Methylene)-p-Phenylenes and Bis(Chloromethylene)-m-Phenylene. *J. Am. Chem. Soc.* **1997**, *119* (52), 12947−12951.
(40) Bhattacharya, D.; Misra, A. Density Functional Theory Based Study of Magnetic Interaction in Bis-Oxoverdazyl Diradicals Connected by Different Aromatic Couplers. *J. Phys. Chem. A* **2009**, *113* (18), 5470−5475.
(41) Tanimoto, R.; Suzuki, S.; Kozaki, M.; Okada, K. Nitronyl Nitroxide as a Coupling Partner: Pd-Mediated Cross-Coupling of (Nitronyl Nitroxide-2-Ido)(Triphenylphosphine)Gold(I) with Aryl Halides. *Chem. Lett.* **2014**, *43* (5), 678−680.
(42) Haraguchi, M.; Tretyakov, E.; Gritsan, N.; Romanenko, G.; Gorbunov, D.; Bogomyakov, A.; Maryunina, K.; Suzuki, S.; Kozaki, M.; Shiomi, D.; Sato, K.; Takui, T.; Nishihara, S.; Inoue, K.; Okada, K. (Azulene-1,3-Diyl)-Bis(Nitronyl Nitroxide) and (Azulene-1,3-Diyl)-Bis(Iminonitroxide) and Their Copper Complexes. *Chem. - Asian J.* **2017**, *12* (22), 2929−2941.
(43) Tretyakov, E. V.; Ovcharenko, V. I. The Chemistry of Nitroxide Radicals in the Molecular Design of Magnets. *Russ. Chem. Rev.* **2009**, *78* (11), 971−1012.
(44) Votkina, D. E.; Petunin, P. V.; Zhivetyeva, S. I.; Bagryanskaya, I. Y.; Uvarov, M. N.; Kazantsev, M. S.; Trusova, M. E.; Tretyakov, E. V.; Postnikov, P. S. Preparation of Multi-Spin Systems: A Case Study of Tolane-Bridged Verdazyl-Based Hetero-Diradicals. *Eur. J. Org. Chem.* **2020**, *2020* (13), 1996−2004.
(45) Barskaya, I. Y.; Veber, S. L.; Suturina, E. A.; Sherin, P. S.; Maryunina, K. Y.; Artiukhova, N. A.; Tretyakov, E. V.; Sagdeev, R. Z.; Ovcharenko, V. I.; Gritsan, N. P.; Fedin, M. V. Spin-State-Correlated Optical Properties of Copper(II)-Nitroxide Based Molecular Magnets. *Dalt. Trans.* **2017**, *46* (38), 13108−13117.
(46) Sworakowski, J. How Accurate Are Energies of HOMO and LUMO Levels in Small-Molecule Organic Semiconductors Determined from Cyclic Voltammetry or Optical Spectroscopy? *Synth. Met.* **2018**, *235*, 125−130.
(47) Petunin, P. V.; Votkina, D. E.; Trusova, M. E.; Rybalova, T. V.; Amosov, E. V.; Uvarov, M. N.; Postnikov, P. S.; Kazantsev, M. S.; Mostovich, E. A. Oxidative Addition of Verdazyl Halogenides to $Pd(PPh_3)_4$. *New J. Chem.* **2019**, *43* (38), 15293−15301.
(48) Massolle, A.; Dresselhaus, T.; Eusterwiemann, S.; Doerenkamp, C.; Eckert, H.; Studer, A.; Neugebauer, J. Towards Reliable References for Electron Paramagnetic Resonance Parameters Based on Quantum Chemistry: The Case of Verdazyl Radicals. *Phys. Chem. Chem. Phys.* **2018**, *20* (11), 7661−7675.
(49) Tolstikov, S. E.; Tretyakov, E. V.; Gorbunov, D. E.; Zhurko, I. F.; Fedin, M. V.; Romanenko, G. V.; Bogomyakov, A. S.; Gritsan, N. P.; Mazhukin, D. G. Reaction of Paramagnetic Synthon, Lithiated 4,4,5,5-Tetramethyl-4,5-Dihydro-1*H*-Imidazol-1-Oxyl 3-Oxide, with Cyclic Aldonitrones of the Imidazole Series. *Chem. - Eur. J.* **2016**, *22* (41), 14598−14604.
(50) Cai, S.; Chen, C.; Sun, Z.; Xi, C. CuCl-Catalyzed Ortho Trifluoromethylation of Arenes and Heteroarenes with a Pivalamido Directing Group. *Chem. Commun.* **2013**, *49* (40), 4552−4554.
(51) Carlin, R. L. *Magnetochemistry*; Springer: Berlin, Heidelberg, 1986; Vol. *79*. DOI: 10.1007/978-3-642-70733-9.
(52) Sheldrick, G. M. *SHELX-97, Programs for Crystal Structure Analysis* (release 97-2), University of Göttingen: Göttingen, Germany, 1997.
(53) Sheldrick, G. M. SHELXT - Integrated Space-Group and Crystal-Structure Determination. *Acta Crystallogr., Sect. A: Found. Adv.* **2015**, *71* (1), 3−8.
(54) *SADABS*, version 2008-1, Bruker AXS: Madison, WI, 2008.
(55) Spek, A. L. *PLATON, A Multipurpose Crystallographic Tool* (version 10M); Utrecht University: Utrecht, The Netherlands, 2003.
(56) Spek, A. L. Single-Crystal Structure Validation with the Program PLATON. *J. Appl. Crystallogr.* **2003**, *36* (1), 7−13.
(57) Macrae, C. F.; Edgington, P. R.; McCabe, P.; Pidcock, E.; Shields, G. P.; Taylor, R.; Towler, M.; Van De Streek, J. Mercury: Visualization and Analysis of Crystal Structures. *J. Appl. Crystallogr.* **2006**, *39* (3), 453−457.
(58) Becke, A. D. Density-Functional Thermochemistry. III. The Role of Exact Exchange. *J. Chem. Phys.* **1993**, *98* (7), 5648−5652.

(59) Lee, C.; Yang, W.; Parr, R. G. Development of the Colle-Salvetti Correlation-Energy Formula into a Functional of the Electron Density. *Phys. Rev. B: Condens. Matter Mater. Phys.* **1988**, *37* (2), 785−789.
(60) Weigend, F.; Ahlrichs, R. Balanced Basis Sets of Split Valence, Triple Zeta Valence and Quadruple Zeta Valence Quality for H to Rn: Design and Assessment of Accuracy. *Phys. Chem. Chem. Phys.* **2005**, *7* (18), 3297−3305.
(61) Dreuw, A.; Head-Gordon, M. Single-Reference Ab Initio Methods for the Calculation of Excited States of Large Molecules. *Chem. Rev.* **2005**, *105* (11), 4009−4037.
(62) Frisch, M.; Ragazos, I. N.; Robb, M. A.; Bernhard Schlegel, H. An Evaluation of Three Direct MC-SCF Procedures. *Chem. Phys. Lett.* **1992**, *189* (6), 524−528.
(63) Andersson, K.; Malmqvist, P. Å.; Roos, B. O. Second-Order Perturbation Theory with a Complete Active Space Self-Consistent Field Reference Function. *J. Chem. Phys.* **1992**, *96* (2), 1218−1226.
(64) Angeli, C.; Cimiraglia, R.; Evangelisti, S.; Leininger, T.; Malrieu, J. P. Introduction of N-Electron Valence States for Multireference Perturbation Theory. *J. Chem. Phys.* **2001**, *114* (23), 10252.
(65) Nagao, H.; Nishino, M.; Shigeta, Y.; Soda, T.; Kitagawa, Y.; Onishi, T.; Yoshioka, Y.; Yamaguchi, K. Theoretical Studies on Effective Spin Interactions, Spin Alignments and Macroscopic Spin Tunneling in Polynuclear Manganese and Related Complexes and Their Mesoscopic Clusters. *Coord. Chem. Rev.* **2000**, *198* (1), 265−295.
(66) Soda, T.; Kitagawa, Y.; Onishi, T.; Takano, Y.; Shigeta, Y.; Nagao, H.; Yoshioka, Y.; Yamaguchi, K. Ab Initio Computations of Effective Exchange Integrals for H-H, H-He-H and Mn_2O_2 Complex: Comparison of Broken-Symmetry Approaches. *Chem. Phys. Lett.* **2000**, *319* (3−4), 223−230.
(67) Neese, F. Software Update: The ORCA Program System, Version 4.0. *Wiley Interdiscip. Rev.: Comput. Mol. Sci.* **2018**, *8* (1), 4−9.

https://doi.org/10.1021/jacs.1c02938
J. Am. Chem. Soc. 2021, 143, 8164−8176